Hydrol. Earth Syst. Sci. Discuss., 11, 6637–6674, 2014
www.hydrol-earth-syst-sci-discuss.net/11/6637/2014/
doi:10.5194/hessd-11-6637-2014

Hydrology and Earth System Sciences
Open Access
Discussions

Iron oxidation kinetics and phosphate immobilization along the flow-path from groundwater into surface water

B. van der Grift[1,2], **J. C. Rozemeijer**[2], **J. Griffioen**[1,2], **and Y. van der Velde**[3]

[1]Department of Innovation, Environmental and Energy Sciences – Faculty of Geosciences, Utrecht University, P.O. Box 80115, 3508 TA Utrecht, the Netherlands
[2]Deltares, P.O. Box 85467, 3508 AL Utrecht, the Netherlands
[3]Soil geography and landscape, Wageningen University & Research centre, P.O. Box, Droevendaalsesteeg 4, 6708 PB Wageningen, the Netherlands

Received: 20 May 2014 – Accepted: 9 June 2014 – Published: 23 June 2014

Correspondence to: B. van der Grift (bas.vandergrift@deltares.nl)

Published by Copernicus Publications on behalf of the European Geosciences Union.

Abstract

The retention of phosphorus in surface waters though co-precipitation of phosphate with Fe-oxyhydroxides during exfiltration of anaerobic Fe(II) rich groundwater is not well understood. We developed an experimental field set-up to study Fe(II) oxidation and P immobilization along the flow-path from groundwater to surface water in an agricultural experimental catchment of a small lowland river. We physically separated tube drain effluent from groundwater discharge before it entered a ditch in an agricultural field. Through continuous discharge measurements and weekly water quality sampling of groundwater, tube drain water, exfiltrated groundwater, and ditch water, we investigated Fe(II) oxidation kinetics and P immobilization processes. The oxidation rate inferred from our field measurements closely agreed with the general rate law for abiotic oxidation of Fe(II) by O_2. Seasonal changes in climatic conditions affected the Fe(II) oxidation process. Lower pH and lower temperatures in winter (compared to summer) resulted in low Fe oxidation rates. After exfiltration to the surface water, it took a couple of days to more than one week before complete oxidation of Fe(II) is reached. In summer time, Fe oxidation rates were much higher. The Fe concentrations in the exfiltrated groundwater were low, indicating that dissolved Fe(II) is completely oxidized prior to inflow into a ditch. While the Fe oxidation rates reduce drastically from summer to winter, P concentrations remained high in the groundwater and an order of magnitude lower in the surface water throughout the year. This study shows very fast immobilisation of dissolved P during the initial stage of the Fe(II) oxidation proces which results in P-depleted water before Fe(II) is competly depleted. This cannot be explained by surface complexation of phosphate to freshly formed Fe-oxyhydroxides but indicates the formation of Fe(III)-phosphate precipitates. The formation of Fe(III)-phosphates at redox gradients seems an important geochemical mechanism in the transformation of dissolved phosphate to particulate phosphate and, therefore, a major control on the P retention in natural waters that drain anaerobic aquifers.

HESSD

11, 6637–6674, 2014

1 Introduction

Eutrophication of freshwater ecosystems following high nutrient loads is a widely recognized water quality problem in agricultural catchments. Phosphorus (P) is often a limiting nutrient in wetlands or fresh aquatic ecosystems (Elser et al., 2007; Wassen et al., 2005) and therefore a key parameter in controlling eutrophication. P enters surface waters through point-sources such as waste water treatment plants and non-point sources via surface runoff and exfiltration of soil water and groundwater. Especially, the fate of P in surface waters originating from non-point sources is controlled strongly by biogeochemical nutrient cycling processes at the soil–water interface (Dahm et al., 1998; Reddy et al., 1999; Dunne et al., 2006).

To date, research and policy on P pollution from non-point sources have focused almost entirely on transfer of particulate bound phosphate from agricultural land to surface waters via overland flow or other fast flow paths during storm flow events (Withers and Haygarth, 2007; Sharpley et al., 2008; Jordan et al., 2012). However, several studies in fresh water systems suggested that substantial dissolved-phosphate loads in surface waters may originate from exfiltration of shallow or deep groundwater (Holman et al., 2008; Dahlke et al., 2012; Scanlon et al., 2005). This is especially likely to occur in delta areas (Griffioen, 2006; Hayashi and Yanagi, 2009), where the soil water and shallow groundwater is typically pH-neutral to slightly acid, anoxic, and iron-rich. The anoxic conditions are very suitable to dissolve phosphate in groundwater, which may result in relative high concentrations of dissolved phosphate from natural origin (Griffioen et al., 2013) or from leached manure or fertilizers (Chardon et al., 2007). In contrast, the chemical composition of surface waters in delta areas is normally pH-neutral to slightly alkaline and oxic with low dissolved iron and phosphate concentrations. This difference in chemical composition between groundwater and surface water creates strong redox and pH gradients at the groundwater-surface water interface (Frei et al., 2012; Carlyle and Hill, 2001). At this interface, the oxidation of iron(II) followed by iron(III) hydrolysis and precipitation of iron oxyhydroxides (from here on referred to as

HESSD
11, 6637–6674, 2014

the iron oxidation process) is the dominant chemical reaction (Griffioen, 2006; Gunnars et al., 2002; Kaegi et al., 2010; von Gunten and Schneider, 1991), that determines the fate of many biochemically important solutes that co-precipitate with the iron oxyhydroxides such as PO_4 (Châtellier et al., 2004; Deppe and Benndorf, 2002; Fox, 1989; Lienemann and Perret, 1999; Mayer and Jarrell, 2000; Voegelin et al., 2013) and AsO_4 (Meng et al., 2002; Roberts et al., 2004; Hug and Leupin, 2003).

The mechanisms and rates of the iron oxidation process with associated binding of phosphate are among the key unknowns in P retention processes in surface waters in lowland catchments. The rate of Fe(II) oxidation strongly depends on pH. At neutral pH, it is a fast reaction that is expected to occur within hours when molecular oxygen is not limited (Stumm and Lee, 1961). At pH values around 6, it may take a couple of days before complete abiotic oxidation of Fe(II) occurs. The reaction rate also depends on oxygen concentration and temperature. Spiteri et al. (2006) investigated the effect of O_2 and pH gradients on oxidative precipitation of Fe(II) and subsequent phosphate sorption along a flow-line in a subterranean estuary where groundwater discharges to the sea. Their results showed that the observed O_2 gradient is not the main factor controlling precipitation and that it is the pH gradient at the mixing zone of freshwater (pH 5.5) and seawater (pH 7.9) that causes a sevenfold increase in the rate of oxidative precipitation of Fe(II).

The majority of studies on redox processes and P dynamics focus on mobilization of phosphate by reductive dissolution of Fe oxyhydroxides in riparian zones or wetlands in response to rewetting (Macrae et al., 2011; Maassen and Balla, 2010; Shenker et al., 2005). In contrast, relatively little is known about the oxidation of Fe(II) in the transition zone from groundwater to surface water in lowland delta areas with (periodic) exfiltration of anaerobic groundwater in relation to P retention in surface water. Moreover, as most of the work on Fe(II) oxidation and incorporation of phosphate into Fe(III) precipitates is performed on synthetic media, the kinetics of these processes in the natural environment are poorly known. A better understanding of these processes will improve

HESSD
11, 6637–6674, 2014

our knowledge of P retention mechanisms in surface waters with exfiltration of anaerobic groundwater as driving force.

To study the dynamics in Fe(II) oxidation and P immobilization along the flow-path from groundwater to surface water, we developed an experimental field set-up in an agricultural experimental catchment of a small lowland river (the Hupsel Brook). Previous studies in the Hupsel Brook catchment have demonstrated that the groundwater in the catchment is predominantly anoxic and contains relatively high dissolved P concentrations in a range of 0.3 to 1.0 mg L^{-1} (Rozemeijer et al., 2010a). At the catchment outlet particulate P is, however, the major contributor to the total P concentrations in the surface water (Rozemeijer et al., 2010b). This indicates that transformation from dissolved P in the groundwater to particulate P in the surface water must have occurred.

In this study we aim (1) to measure the dynamics of Fe(II) and phosphate concentrations along the flow-path from groundwater into surface water in a typical lowland catchment in the Netherlands (2) to infer reaction rates and mechanisms that influence the iron oxidation process by a combination of data analysis and chemical modelling and (3) to explore the phosphate immobilization process during the flow of anaerobic iron-rich groundwater towards surface water.

2 Methods

2.1 Study area

An experimental set-up was installed in the Hupsel Brook agricultural lowland catchment, the Netherlands (Fig. 1) (52°03′ N, 6°38′ E). The size of this catchment is 6.64 km^2, with altitudes ranging from 22 to 36 m a.m.s.l. (above mean sea level). A weather station of the Royal Dutch Meteorological Institute (KNMI, De Bilt, the Netherlands) is located within the catchment. The Hupsel brook catchment has a moderate maritime climate with an average annual temperature of 9.5 °C and average annual precipitation of 770 mm. Our field-scale experiment location in the Hupsel

HESSD
11, 6637–6674, 2014

catchment is a 9000 m^2 tube drained meadow dominated by the grass Lolium perenne; surface elevation ranges from 28 to 31 m a.m.s.l. and a ditch (average depth of 1.2 m below soil surface) borders the field at the eastern side. This ditch drains a sub-catchment of the Hupsel Brook as indicated in Fig. 1. The direction of the groundwater flow in the field is from northwest to southeast. The groundwater drains towards the eastern ditch or flows into the adjacent field south of the experimental field (Rozemeijer et al., 2010c). The drainage tubes are separated 14.5 m from each other and discharge into the eastern ditch at 90 cm depth. To separate the water fluxes of different flow routes towards the eastern ditch, three adjacent sheet pile reservoirs were built in the ditch (Fig. S1 in the Supplement). These in-stream reservoirs were constructed around single drainage outlets and stretched along 43.5 m of the field. The wooden sheet piles were driven into an impermeable 30 m thick Miocene clay layer starting at a depth of 3 to 5 m to capture all groundwater flow from the field into the ditch. The in-stream reservoirs captured overland flow, interflow, direct precipitation, and groundwater flow from the thin, phreatic aquifer above the Miocene clay layer. The water levels in the reservoirs were measured continuously with pressure sensors from November 2007 to October 2008. The water levels inside the in-stream reservoirs were maintained at the ditch water level by pumps. Excess water was pumped from the in-stream reservoirs into the ditch, and the pumped volumes were recorded with digital flux meters (Van der Velde et al., 2010). The water flow from the individual tube drains was separated from the other flow routes by connecting each drain to a 500 L vessel. Water from these vessels was pumped into the ditch and volumes were measured with water flux meters (Van der Velde et al., 2010).

Four groundwater wells were installed for sampling of groundwater in a transect across the experimental field parallel to the ditch at a distance of 20 m from the ditch. The filters of the wells were installed 2–3 m below the surface. More detailed information about the Hupsel catchment and all installations and measurements is found in Van der Velde et al. (2010).

HESSD
11, 6637–6674, 2014

2.2 Water quality measurements

We collected water samples from the four groundwater wells, the three tube drains and the three in-stream reservoirs from May 2007 until December 2008. In addition surface water samples were taken from the sub-catchment outlet and the catchment outlet. All samples were taken weekly using a peristaltic pump. During the dry summer period (July to October), the tube drains and in-stream reservoirs occasionally ran dry and sampling was sometimes not possible. We reduced the sampling to a biweekly scheme during this period. The samples were filtered in situ (0.45 µm) and Temperature and pH were measured immediately in the field. The samples were analyzed for metals, nutrients and anions within 48 h using Ion Chromatography (NO_3, SO_4, Cl), ICP-AES (Na, K, Ca, Fe, Mg, Si), ICP-MS (P, Al) and AA3 (Automated Segmented Flow Analyzer) (NH_4). Alkalinity was measured by titration. We used a variable span smoother based on local linear fits (Friedman, 1984) to aggregate trends trough the concentration measurements.

2.3 Modeling reaction kinetics

To test the validity of existing chemical models developed under laboratory condition for the oxidation of Fe and co-precipitation of PO_4 for our field situtaion, we modelled the Fe and PO_4 concentrations in the reservoirs with PHREEQC (Parkhurst and Appelo, 1999) with the WATEQ4F database (Ball and Nordstrom, 1991) using the representative aqeous composition of the groundwater (Table S1 in the Supplement). First, the Fe concentrations in the reservoirs were described as a first-order reaction process following the general rate law for homogeneous chemical oxidation of Fe(II) by O_2 in laboratory systems:

$$-\frac{\mathrm{dFe(II)}}{\mathrm{d}t} = K[\mathrm{Fe(II)}][\mathrm{OH}^-]^2 pO_2 \quad (1)$$

HESSD
11, 6637–6674, 2014

with a value for the abiotic rate constant K at 20 °C of $7.9(\pm 2.47)\times 10^{13}$ M^{-2} atm^{-1} min^{-1} (Stumm and Lee, 1961). Now by assuming a continous stirred tank reactor (CSTR) with perfect mixing and steady-state concentrations, we can describe Fe(II) concentrations in the reservoir as function of transit times of water through the reservoirs (Perry et al., 1997):

$$Fe_r = \frac{Fe_i}{1 + (k \cdot \overline{T})} \quad (2)$$

where Fe_r is the Fe(II) concentration of the water in the reservoir, Fe_i is the Fe(II) concentration of the groundwater that flows into the reservoir, k is the rate constant according Eq. (1) and $\overline{T}$ is the mean transit time.

The mean transit time $\overline{T}$, of the water leaving the reservoirs at time t can be approximated through the assumption of fully mixed reservoirs with a variable flow ($q(t)$) and volume ($V(t)$), following (Botter et al., 2011):

$$\overline{T}(t) = \int_{\theta}^{\infty} \frac{q(t-T)}{V(t-T)} e^{-\int_0^T \frac{q(t-T+\tau)}{V(t-T+\tau)} d\tau} \cdot T \, dT \quad (3)$$

where $q(t-T)$ is the reservoir discharge and $V(t-T)$ is the reservoir volume at time t that has been inside the reservoir (i.e. the transit time) for a period T.

In a second step, the uptake of phosphate to Fe precipitates was modelled with two models using different concepts. First, surface complexation to ferrihydrite was considered using the Dzombak and Morel (1990) model. Surface complexation of carbonate and silicate to ferrihydrite was included, using the stability constants of Van Geen et al. (1994) and Bonte (2013). Second, precipitation of a ideal solid-solution between amorphous Fe hydroxide and strengite ($Fe(III)PO_4$) was considered (Griffioen, 2006).

HESSD
11, 6637–6674, 2014

3 Results

3.1 Fe concentrations

The groundwater samples (Fig. 2a) had Fe concentrations ranging between 0.2 and 45.5 mg L^{-1} with an average of 15.9 mg L^{-1} and a median value of 14.5 mg L^{-1}. The groundwater showed a temporal and spatial variation in Fe concentrations, but they were generally higher than in the other water types. The measured groundwater concentrations are common values for anaerobic groundwater in the eastern part of the Netherlands (Vermooten et al., 2008).

The tube drain water samples (Fig. 2b) had Fe concentrations ranging between 0.4 and 18.9 mg L^{-1} with an average of 4.5 mg L^{-1} and a median value of 1.9 mg L^{-1}. The Fe concentrations of tube drains 1 and 2 were for the majority of samples lower than 2 mg L^{-1}. At some moments in the winter months of 2007–2008 tube drain 2 had Fe concentrations around 5 mg L^{-1}. Tube drain 3 showed a large change in Fe concentration: the Fe concentrations increased from values around 2 mg L^{-1} to values between 10 and 15 mg L^{-1} during the period September–November 2007 and exceeded 15 mg L^{-1} in November and December 2008. This water approached the Fe concentrations of the groundwater. A change in concentration of redox-sensitive components like NO_3, NH_4, Mn, As, HCO_3 was also observed in the drain 3 water (not shown).

The reservoir water samples (Fig. 2c) had Fe concentrations ranging between 0.1 and 34.6 mg L^{-1} with an average of 3.9 mg L^{-1} and a median value of 2.0 mg L^{-1}. There was a winter peak in the Fe concentration of the in-stream reservoirs. During the winter (November–February), the Fe concentration reached the level of the Fe concentrations of the groundwater (5–35 mg L^{-1}), while in summer season (April–September) a majority of samples had Fe concentrations lower than 5 mg L^{-1} with an average of 1.76 mg L^{-1}. The range and average of the Fe concentrations differed between the three reservoirs during the winter period (Table 1). Reservoir 2 showed the highest concentrations followed by reservoir 3 and subsequently reservoir 1. Likely, this was the result of spatial variation of Fe concentrations in the groundwater, where reservoir

HESSD
11, 6637–6674, 2014

2 and 3 drained groundwater with higher Fe concentrations than reservoir 1. On average, groundwater wells 1 and 2 had the highest Fe concentrations (Fig. 2a). As the direction of the groundwater flow in the experimental field is roughly from northwest to southeast (Fig. 1), it is conceivable that this Fe-rich groundwater flows into reservoir 2 and 3.

The surface water samples (Fig. 2d) had Fe concentrations ranging between 0.15 and 2.21 mg L^{-1} with an average of 0.68 mg L^{-1} and a median value of 0.60 mg L^{-1}. There was no seasonal variation and no difference between the sub-catchment outlet and catchment outlet.

3.2 P concentrations

The dissolved P concentrations of the groundwater were an order of magnitude higher than that of the tube drain water, reservoir water and surface water (Fig. 3). Where the median P concentration equaled 0.33 mg L^{-1} in the groundwater, it was around 0.02 mg L^{-1} for all other water types. Despite some short-scale temporal variation in the P concentration at individual groundwater wells, the data showed increased P concentrations during summer (Fig. 3a) (we did not investigate this further).

There was an increase in P concentration at tube drain 3 starting in November 2007 (Fig. 3b). This was two months after the increase of Fe (Fig. 3b). However, the P concentration at tube drain 3 after the redox transition did not reach the level of the P concentration of anaerobic groundwater (Fig. S3 in the Supplement).

There was no clear seasonal trend in P concentrations in the reservoirs and surface water (Fig. 3c and d). Note that the Fe concentrations of the reservoir water in winter time almost matched that of the anaerobic groundwater but the P concentrations were an order of magnitude lower.

HESSD
11, 6637–6674, 2014

3.3 Supporting variables

Following Eqs. (1) and (2), Fe concentrations can be explained from, pH, temperature, oxygen pressure of the water and the transit time of water inside the reservoirs. These variables have been measured directly or approximated. There was a seasonal variation in the pH of the water in the reservoirs (Fig. 4). The pH varied between 6 and 6.5 with an average of 6.16 during the cold November to March. Although the sampling frequency was lower during the warmer April to October, the majority of samples had pH values above 6.5 with an average of 6.6. The temperature of the ditch water varied between 2.7 and 21.5 °C (Fig. 5). Complete or almost complete oxygen saturation of the water in the reservoirs seems to be reasonable due to the following reasons: the water in the reservoirs was in direct contact with the atmosphere; the water depth varied between a few and approximately 40 cm; during 93 % of time period of the experiment the transit time of the water in the reservoirs was longer than one day (see next paragraph); there were no visual indications of stratification in the reservoirs throughout the year.

3.3.1 Reservoir transit time

To explore Fe oxidation kinetics and P immobilization during exfiltration on anaerobic groundwater to surface water we calculated the mean transit time of the exfiltrated groundwater in the reservoirs from the reservoir discharge and the reservoir volume according Eq. (3). The reservoir discharge, and therefore, the groundwater inflow into the reservoirs showed an decrease from winter to summer (Van der Velde et al., 2010). The reservoir volumes decreased as well but to a lesser extent than the reservoir volume (Supplement S1). This resulted in an increase of the mean transit time of the water in the reservoirs. The transit time varied between 2 and 6 days during the period November 2007–March 2008 (Fig. 5) with longer transit times during relatively short, drier periods and transit times shorter than 2 days during the intensive discharge peaks. From April 2008 to December 2008 the variation in transit time was larger compared to the period November 2007–March 2008. Transit times longer than 8 days were common

HESSD
11, 6637–6674, 2014

in the period from April 2008 to December 2008. During dry periods the transit time increased gradually up to 20 days. Precipitation events following these dryer periods reduced the transit time immediately to a few days. During five events in the summer of 2008 reservoir 1 felt dry and, therefore, no transit time could be calculated.

4 Discussion

4.1 Behavior of Fe

The first objective of our study was to measure the dynamics of Fe concentrations along the flow path from groundwater into surface water. The Fe concentrations of the reservoir water and tube drain water were dynamic over the year. The higher Fe concentrations of the reservoir water during winter time suggest that only a part of the Fe(II) in the groundwater that was leached into the reservoirs was oxidized at the time of sampling. In summer time, the dissolved Fe concentrations of the water in the reservoirs are low, indicating that Fe(II) is completely oxidized prior to inflow into the reservoirs.

4.1.1 Reservoirs

The Fe concentrations of the reservoir water depend on the rate of the Fe oxidation process in combination with the flux of Fe-rich groundwater into the reservoirs and the transit time in the reservoirs. The pH, oxygen concentration and temperature are the major controls on the Fe(II) oxidation rate. The difference in maximum and minimum temperature of the ditch water is almost 20 °C (Fig. 5). A tenfold increase of the rate upon raising the temperature by 15 °C is reported for abiotic oxidation of Fe(II) by oxygen (Sung and Morgan, 1980). This is mainly caused by the change in OH^- concentration due to the temperature dependence of the ionization constant of water.

There was a seasonal variation in the pH of the water in the reservoirs (Fig. 4), with lower values in winter and higher values in summer. According to the rate law for abiotic

HESSD
11, 6637–6674, 2014

Fe(II) oxidation Eq. (3), a drop of half a pH unit for pH around 6–7 results theoretically in a nine-fold increase in the half-life time of Fe(II). Therefore, the seasonal variation in the pH is another control on the dynamics in the Fe concentration of the reservoirs water. The smaller seasonal variation in the pH and Fe concentration in reservoir 1 compared to reservoir 2 and 3 supports this conclusion.

Seasonal changes in pH may be induced by CO_2 degassing of surface water or by photosynthesis in the surface water column (House and Denison, 1997; Neal et al., 2002). The average pCO_2 of all groundwater samples is 0.056 atm. For the reservoir water during the summer months and winter months this is 0.024 and 0.048 atm respectively. Degassing of CO_2 is kinetically controlled and, therefore, it may take a couple of days before equilibrium with air is reached. Obviously, photosynthesis occurs mainly during summer months. So, we assume that longer transit times and higher temperatures of the water in the reservoirs during summer months compared to the winter months resulted in more extensive CO_2 degassing. This resulted into higher pH values during summer. In contrast to CO_2 degassing, hydrolysis following oxidation of Fe(II) to Fe(III) generates acidity. This reduces the alkalinity of water and tempers the pH increase following CO_2 degassing. Modelling calculations with PHREEQC indicated that oxygenation and degassing groundwater with a pH or 6.16, Fe(II) concentration of 15.9 mg L^{-1}, and pCO_2 of 0.056 atm to the summer-average pCO_2 of the reservoir water of 0.024 atm results in pH values of 6.54 and 6.39 without and with oxidative hydrolysis, respectively.

The transit time of the water in the reservoirs also explains the low Fe concentrations in the summer months. Figure 6a shows that the measured concentrations decrease with an increase of the mean transit time, although a large variation of the Fe concentrations around the variable span smoother exists. Iron concentrations higher than 5 mg L^{-1} were only found at moments on which the residence time was less than 5 days. Samples from November to February have predominantly residence times shorter than 5 days and Fe concentrations above the smoother line. The Fe

HESSD
11, 6637–6674, 2014

concentrations of samples from March to October were predominantly lower than the smoother line.

4.1.2 Tube drains

The increase in Fe concentration of tube drain 3 indicates a change in the redox status of the drained water. The flow data of the tube drains showed a decrease of the discharge rate of drain 3 starting in December 2007 (Fig. S4 in Supplement). This indicates that the redox change was caused by clogging of the tube drain due to precipitation of Fe oxyhydroxides in combination with the growth of microbial biomass in the tube drain. Clogging results in an increase of the water saturation of the tube drain and therefore in a decrease of atmospheric oxygen penetration in the tube drain itself and the surrounding soil. The Fe oxidation, therefore, no longer occurs in the tube drain or the surrounding soil but after groundwater is discharged to the surface water. Clogging of filter material at redox boundaries is a common phenomenon for example in drilled wells for groundwater abstraction and also tube drains (Houot and Berthelin, 1992; Van Beek et al., 2009; Wolthoorn et al., 2004).

4.1.3 Surface water

Unlike the water in the reservoirs, the Fe concentrations of the water at the sub-catchment outlet and the catchment outlet were year-round close to zero. This indicates that the Fe(II) from the groundwater is completely oxidized at these locations. The absence of water with Fe concentrations in the range of the reservoir water is explained by the longer residence time of the surface water at the sub-catchment and catchment outlet and by contributions of the dominantly aerobic Fe-depleted tube drain water to the surface water discharge. Tube drain water was physically separated from the groundwater at our experimental field and, therefore, did not contribute to the inflow to the reservoirs. Van der Velde et al. (2010) concluded that during normal flow

HESSD
11, 6637–6674, 2014

conditions, the tile drain contribution to surface water discharge is more important than the groundwater contribution.

Although close to zero, the Fe concentrations of the surface water samples were higher than concentrations predicted by assuming equilibrium of Fe(III) with a Fe oxyhydroxide phase. The presence of this additional dissolved Fe has been variously attributed to Fe(III) in colloidal phases (Lyvén et al., 2003) or complexed Fe(II) (Lofts et al., 2008). The particulate colloidal Fe(III) can exist as both organic complex and small hydroxide particle (Lyvén et al., 2003; Allard et al., 2004; Benedetti et al., 2003). Colloidal Fe(III) is stabilized against aggregation by binding of dissolved organic carbon (DOC) on its surface. Neal et al. (2008) found positive correlations between Fe and DOC concentrations of river water.

4.2 Fe oxidation kinetics

The second objective of our study was to infer reaction rates and mechanisms that influence the Fe oxidation process. The kinetic oxidation of dissolved Fe(II) was modeled according the general rate law as reported by Stumm and Lee (1961). The Fe oxidation rates inferred from our field measurements closely agree with the general rate law for abiotic oxidation of Fe(II) by O_2 ($k = 7.9 \times 10^{13}\,M^{-2}\,atm^{-1}\,min^{-1}$) (Fig. 6a). Seasonal changes in pH and temperature of the reservoir water had a major effect on the Fe(II) oxidation rate as explained below.

The grey lines in Fig. 6a represents the steady-state Fe(II) concentration as function of the transit times as calculated with the CSTR-model. The model simulates the Fe(II) oxidation in the reservoirs for the yearly average conditions, a typical summer situation, and a typical winter situation. Table 2 gives the input parameters for the CSTR model. The Fe concentration of the groundwater (Fig. 2a) was used as inflow concentration (Fe_i in Eq. 2) to the reservoir. This is variable in space and time between 0.2 and 40 mg L^{-1}. Because we do not know the values of Fe_i at sampling moments exactly, it was not possible to derive field-based oxidation rates for the individual measured Fe concentrations. The Fe concentration of the groundwater that flows into the reservoirs

HESSD
11, 6637–6674, 2014

(Fe_i) was set to 14.5 mg L^{-1} representing the median concentration of Fe in the groundwater. The median concentration was preferred above the average concentration due to the skewness of the Fe concentration distribution to high values. The thin lines in Fig. 6a represent a typical summer and winter situation. The Fe_i for the summer and winter situations were set to the 25-percentile and 75-percentile of Fe concentration in the groundwater (10.6 and 21.3 mg L^{-1}, respectively). The input values for the rate controlling parameters were assigned as follows: (1) the pH values are the yearly averaged and seasonally averaged values of the reservoir water samples (6.4, 6.2 and 6.6, respectively), (2) for dissolved oxygen in the winter situation we assume that the equilibrium time to reach complete saturation is less than the half-life time of Fe(II). Therefore, we used complete oxygen saturation (pO_2 = 0.21 atm) for the winter situation. The Fe(II) oxidation rate is clearly higher in the summer situation. The Fe(II) is presumably completely oxidized before the reservoir water is in equilibrium with atmospheric oxygen. For this reason we modelled the reaction for the summer situation with a pO_2 of 0.1 atm, (3) the temperature for the yearly average model was set to the yearly averaged temperature of the ditch water (9.3 °C) and to 17 and 5 °C for the summer and winter situation respectively (Fig. 5).

Although microbial Fe(II) oxidation at low oxygen concentration and autocatalytic Fe(II) oxidation due to adsorption of Fe(II) onto surfaces of previously formed Fe oxyhydroxides may happen in the reservoirs, enhanced reaction rates caused by these processes were not considered in our model. Autocatalytic Fe(II) oxidation is only observed in experiments with a pH of 7 and higher (Sung and Morgan, 1980). The pH of the reservoir water never reached this value. Moreover, Vollrath et al. (2012) argue that the rate law originally proposed by Stumm and Lee (1961) was already influenced by surface catalysis and, therefore, not strictly represents homogeneous Fe(II) oxidation.

Figure 6a shows that the variable span smoother through the observations matches with the model for the year average conditions. Therefore we conclude that the decrease of the Fe concentration with increasing transit time of the water in the reservoirs closely agreed with the reported rate law of abiotic Fe(II) oxidation in laboratory

HESSD
11, 6637–6674, 2014

systems with a rate constant of $7.9 \times 10^{13}\,M^{-2}\,atm^{-1}\,min^{-1}$ (Stumm and Lee, 1961). Most measured Fe concentrations fall between the summer-type and winter-type lines. The winter-type model seems to underestimate the Fe(II) oxidation rate slightly. This is likely due to microbial Fe(II) oxidation that become increasingly important when abiotic rates are retarded by low temperatures (de Vet et al., 2011), like in our winter situation. The large difference between the summer-type and winter-type model illustrates the effect of the temperature and pH on the abiotic Fe(II) oxidation rate. Figure 6a makes clear that the oxidation of Fe in anaerobic groundwater after being discharged to surface water is not instantaneous. It will take a couple of days to more than one week before complete oxidation of Fe(II) is reached, especially under winter conditions.

4.3 Behavior of P

The third objective was to measure the dynamics in P concentrations and to explore the phosphate immobilization process during flow of anaerobic iron-rich groundwater towards surface water. Our field data show that dissolved P preferentially precipitates from solution during the initial stage of the Fe(II) oxidation process. When high Fe concentrations happened in the reservoir water and the water from tube drain 3, substantially lower P concentrations were found in these waters compared to the groundwater. The average molar P/Fe ratios of the reservoir water and tube drain 3 varied between 0.004 and 0.014 during winter time (Table 1); this is distinctly lower than the P/Fe ratio in the groundwater that varied between 0.016 and 0.079. A single Fe-oxide flocs sample from a drain had a molar P/Fe ratio of 0.033. This is in the range of the groundwater P/Fe ratio. Moreover, there is no relation between the P concentration of the reservoir water and the transit time (Fig. 6b) and no clear seasonal dynamics in P concentrations in the waters other than groundwater exist (Fig. 3). For tube drain 3, two mechanisms might cause these observations: (1) the average P concentration of the anaerobic groundwater that flowed into the tube drain was lower than the groundwater sampled from the four wells or (2) there was continuous immobilization of dissolved

HESSD
11, 6637–6674, 2014

P in tube drain 3 despite the observation that complete oxidation of Fe no longer occurred in this drain. For the reservoirs, it is not likely that the inflow of groundwater with low P concentrations determined the P concentration of this water. After all, the groundwater was sampled from four wells parallel to the reservoirs covering almost the entire stretch of the reservoirs. So the observations point to a rapid transformation of dissolved P to particulate P during the initial stage of Fe(II) oxidation along the flow-path of groundwater into surface water. This resulted in P-depleted water before Fe(II) was depleted.

The black and blua lines in Fig. 6b are the steady-state P concentration according to the two CSTR-models for phosphate immobilisation as function of the transit time. The models simulates the binding of phosphate by surface complexation to Fe oxyhydroxide precipitates that formed during Fe(II) oxidation and precipitation of an solid solution between amorphous Fe hydroxide and strengite ($Fe(III)PO_4$). The P concentrations of the inflow water were set to 0.33, 0.52 and 0.19 $mg\,L^{-1}$ representing the median, 75-percentile and 25-percentile of P concentration in the groundwater (Table 2). Figure 7b indicates clearly that the measured P concentrations are distinctly lower than de concentrations according to the surface complexation model for the whole range of transit times. The immobilisation of P during aeration of groundwater could not solely be attributed to surface complexation to a Fe-oxide type of phase. The concentrations according to the model that simulate the presipitation of a solid-solution between amorphous Fe hydroxide and strengite ($Fe(III)PO_4$) are in the range of the measured concentrations. The variable span smoother through the observations matches with the model for the year average conditions. The the fast immobilisation of P during the short transit times, where Fe(II) was still present in high concentration, could satisfactory be described by the model. This indicates the formation of Fe(III)-phosphate precipitates during the initiail stage of Fe(II) oxidation until phosphate is depleted from solution. The model overestimates the lowest measured P concentration. This could be attributed to additional adsorption of phosphate to the Fe-oxides that were as well formed in the solid-solution or by uncertainty in the logK value of strengite.

HESSD
11, 6637–6674, 2014

Recently, Voegelin et al. (2013) studied the effect of phosphate on the formation of Fe precipitates upon oxidation of Fe(II) at near-neutral pH. Their data verifies that Fe(II) oxidation initially results in the precipitation of a phosphate-rich Fe-precipitate whose P/Fe ratio reaches ~ 0.52 at the time of near-complete phosphate depletion from solution. This is supported by a limited number studies (Deng, 1997; Gunnars et al., 2002) which indicated that during Fe(II) oxidation in solutions with initial dissolved P/Fe ratio less than ~ 0.5, a phosphate-rich precipitate with molar P/Fe ratio of ~ 0.5–0.6 forms first. Rather than a simple formation of Fe(III)-hydroxide coupled with competitive ion adsorption, Voegelin et al. (2013) concluded that several types of Fe(III)-precipitates may form and transform over the course of Fe(II) oxidation in the presence of phosphate. Fe(III)-phosphate, phosphate-saturated hydrous ferric oxide, goethite and lepidocrocite were successively formed in their study depending on the dissolved molar P/Fe ratios. The observations from our experimental field site are thus supported by laboratory experiments on synthetic samples.

4.4 Dynamics in the redox gradient

The higher Fe concentration of the reservoir water during winter compared to summer are explained by a reduction of the Fe(II) oxidation rate combined with an increased inflow of groundwater into the reservoirs. Based on our data, we argue that the oxidation rate of Fe(II) in combination with groundwater inflow to the ditch is such that the Fe(II) oxidation occurs at the sediment–water interface or deeper in the soil domain during summer, resulting in low Fe(II) concentrations of the reservoir water (Fig. 3). Fe(II) oxidation shifts to the surface water in winter evidenced by high Fe(II) concentrations. This argument is supported by visual observations of the ditch water during the field experiment. The easily resuspendable Fe-oxide flocs which have sedimented on ditch bottoms were predominantly found in winter time (Fig. 7). So, the position of the redox gradient in the groundwater-surface water interface of our experimental field is dynamic in time as a result of dynamics in hydrological and biogeochemical conditions. Krause et al. (2009) measured highly complex temporal changes in redox status and

HESSD
11, 6637–6674, 2014

pore water nitrate concentrations at the sediment-interface. Maassen and Balla (2010) measured the effect of these redox dynamics on phosphorus mobilization to surface water. We show that this as well may impact the phosphorus immobilization during from groundwater to surface water.

Due to deeper groundwater tables in summer oxygen-saturated surface water may start to infiltrate and atmospheric oxygen may penetrate the soil surrounding the tube drains. Through higher groundwater tables and more discharge this oxygen-saturated water is flushed out again in winter time. Moreover, the abundant growth of grasses and reeds inside the ditches is likely to actively transfer oxygen through the groundwater-surface water interface during summer time. In a previous experiment at the same field site an iron-rich zone was observed directly around the drain tube, causing an orange-colored "ring" in the soil around the tube drain (Van den Eertwegh, 2002). The P content of the solid material in this ring was three times higher than for soil samples taken just outside this iron-rich zone.

4.5 Suspended sediment

The formation of Fe-oxide flocs in the surface water contributes to the suspended sediment concentration of this surface water. The origin of suspended sediments and particulate-bound P in agricultural catchments is widely studied (Ballantine et al., 2008; Walling et al., 2008). Traditionally, two source types of suspended sediment are being distinguished: surface erosion and resuspension of streambed sediment. Rainstorm events and high discharge peaks are commonly considered as the trigger for mobilization of these source materials (Horowitz, 2008). Little attention has been paid to the formation of authigenic sediment in the surface water systems formed by exfiltration and oxygenation of anaerobic groundwater. However, we argue that it may be an important suspended sediment source in areas draining anaerobic groundwater. The only studies, known to us, on authigenic sediments in freshwater systems formed by oxidation of iron-rich groundwater are from Baken et al. (2013) and Vanlierde et al. (2007). They reported an average annual authigenic mineral contribution

HESSD
11, 6637–6674, 2014

to the total suspended sediment flux between 31 and 75 % for a catchment in Belgium. Based on the Hupsel field experiment data, we argue that the formation of authigenic suspended sediments in the surface water domain predominantly occurs in winter time and that this attributes to an increase in the turbidity of surface water combined with a change in colour of the surface water compared to the summer situation.

4.6 Remobilization of phosphate

Finally, the question arises what the effect of the preferential P precipitation during oxidation of Fe(II) will be on phosphate retention. The formation of Fe(III)-phosphate precipitates during oxygenation of groundwater in the soil surrounding the ditch or tube drain may result in permanent retention of phosphate at the transition zone from groundwater to surface water. However, the particulate P stored in this zone may be discharged to the surface water by erosion during high flow conditions or remobilized to dissolved P by reductive dissolution or aging of Fe(III) precipitates. Thus, the transformation of the Fe precipitates may result in the release of dissolved phosphate. A limited number of time-resolved experiments addressed the effect transformation processes. Voegelin at al. (2013) measured a slow increase in dissolved phosphate after most Fe(II) had been oxidized. Gerke (1993) found that about 38 % of the phosphate adsorbed to freshly-prepared ferrihydrite was released back into solution within 38 days of aging. Mayer and Jarrell (2000) observed ~ 75 % phosphate release back into solution after 10–15 days of aging. Voegelin et al. (2013) attributed this phosphate release to ongoing Fe(III) polymerization into (crystalline) Fe(III)-(hydr)oxides combined with no further Fe(III) supply to the solid phase that could have retained phosphate. The question remains if this phosphate release process due to aging of minerals occurs in the natural environment as well at these reported levels. After all, there is an ongoing Fe(II) supply in the natural environment resulting in the formation of new Fe(III) precipitates. Moreover, solutes such as silicate or humic acid interfer with Fe(III) polymerization and may markedly slow down Fe(III) polymerization, phase transformation and associated phosphate release (Gerke, 1993; Mayer and Jarrell, 2000).

HESSD
11, 6637–6674, 2014

5 Conclusions

This field study demonstrates that: (1) the Fe concentrations of water in in-stream reservoirs capturing exfiltrating anaerobic groundwater and the tube drain water were dynamic over the year. The Fe concentrations of the water in the reservoirs were high and reached the levels of the groundwater in winter time and were low in summer time. This indicates seasonal changes in the Fe(II) oxidation rate. The dissolved P concentration of the reservoir water and tube drain water were an order of magnitude lower than observed in the groundwater throughout the year. Seasonal changes in the Fe(II) oxidation rate had no impact on the P immobilization, (2) the Fe(II) oxidation rate at our field site closely agrees with reported rate laws for abiotic oxidation of Fe(II) by O_2. Due to lower a pH and temperature the Fe(II) oxidation rates are lower in winter time compared to summer time. Combined with higher groundwater fluxes during winter this likely resulted in a shift from Fe(II) oxidation occuring in the soil or ditch sediment in summer time to the surface water in winter time, (3) the exfiltrating groundwater is depleted in dissolved phosphate before Fe(II) is depleted. The P immobilization at our field site is much faster than can be explained by the surface complexation model proposed by Dzombak and Morel (1990). The fast P immobilization could satisfactory be described with the precipitation of an solid-solution between amorphous Fe hydroxide and strengite (Fe(III)-phoshpate). The formation of Fe(III)-phosphates at redox gradients seems to be an important biogeochemical mechanism in the transformation of dissolved phosphate to particulate phosphate and, therefore, a major control on the phosphate retention in streams and ditches that drain anaerobic groundwater.

The Supplement related to this article is available online at doi:10.5194/hessd-11-6637-2014-supplement.

HESSD
11, 6637–6674, 2014

References

Allard, T., Menguy, N., Salomon, J., Calligaro, T., Weber, T., Calas, G., and Benedetti, M. F.: Revealing forms of iron in river-borne material from major tropical rivers of the Amazon Basin (Brazil), Geochim. Cosmochim. Ac., 68, 3079–3094, doi:10.1016/j.gca.2004.01.014, 2004.

Baken, S., Sjöstedt, C., Gustafsson, J. P., Seuntjens, P., Desmet, N., De Schutter, J., and Smolders, E.: Characterisation of hydrous ferric oxides derived from iron-rich groundwaters and their contribution to the suspended sediment of streams, Appl. Geochem., 39, 59–68, doi:10.1016/j.apgeochem.2013.09.013, 2013.

Ball, J. W. and Nordstrom, D. K.: User's Manual for WATEQ4F, with revised thermodynamic data base and text cases for calculating speciation of major, trace, and redox elements in natural waters, Menlo Park, California, United States, U.S. Geological Survey, 1991.

Ballantine, D. J., Walling, D. E., Collins, A. L., and Leeks, G. J. L.: The phosphorus content of fluvial suspended sediment in three lowland groundwater-dominated catchments, J. Hydrol., 357, 140–151, 2008.

Benedetti, M. F., Ranville, J. F., Allard, T., Bednar, A. J., and Menguy, N.: The iron status in colloidal matter from the Rio Negro, Brasil, Colloid. Surface. A, 217, 1–9, doi:10.1016/S0927-7757(02)00553-8, 2003.

Bonte, M.: Impacts of Shallow Geothermal Energy on Groundwater Quality – a Hydrochemical and Geomicrobial Study of the Effects of Ground Source Heat Pumps and Aquifer Thermal Energy Storage, Ph.D. thesis, Vrije Universiteit Amsterdam, Amsterdam, the Netherlands, 2013.

Botter, G., Bertuzzo, E., and Rinaldo, A.: Catchment residence and travel time distributions: the master equation, Geophys. Res. Lett., 38, L11403, doi:10.1029/2011GL047666, 2011.

Carlyle, G. C. and Hill, A. R.: Groundwater phosphate dynamics in a river riparian zone: effects of hydrologic flowpaths, lithology and redox chemistry, J. Hydrol., 247, 151–168, 2001.

Chardon, W. J., Aalderink, G. H., and Van Der Salm, C.: Phosphorus leaching from cow manure patches on soil columns, J. Environ. Qual., 36, 17–22, 2007.

Châtellier, X., West, M. M., Rose, J., Fortin, D., Leppard, G. G., and Ferris, F. G.: Characterization of iron-oxides formed by oxidation of ferrous ions in the presence of various bacterial species and inorganic ligands, Geomicrobiol. J., 21, 99–112, 2004.

HESSD
11, 6637–6674, 2014

Dahlke, H. E., Easton, Z. M., Lyon, S. W., Todd Walter, M., Destouni, G., and Steenhuis, T. S.: Dissecting the variable source area concept – subsurface flow pathways and water mixing processes in a hillslope, J. Hydrol., 420–421, 125–141, 2012.

Dahm, C. N., Grimm, N. B., Marmonier, P., Valett, H. M., and Vervier, P.: Nutrient dynamics at the interface between surface waters and groundwaters, Freshwater Biol., 40, 427–451, doi:10.1046/j.1365-2427.1998.00367.x, 1998.

de Vet, W. W. J. M., Dinkla, I. J. T., Rietveld, L. C., and van Loosdrecht, M. C. M.: Biological iron oxidation by Gallionella spp. in drinking water production under fully aerated conditions, Water Res., 45, 5389–5398, 2011.

Deng, Y.: Formation of iron(III) hydroxides from homogeneous solutions, Water Res., 31, 1347–1354, 1997.

Deppe, T. and Benndorf, J.: Phosphorus reduction in a shallow hypereutrophic reservoir by in-lake dosage of ferrous iron, Water Res., 36, 4525–4534, doi:10.1016/S0043-1354(02)00193-8, 2002.

Dunne, E. J., Reddy, K. R., and Clark, M. W.: Phosphorus release and retention by soils of natural isolated wetlands, Int. J. Environ. Pollut., 28, 496–516, 2006.

Dzombak, D. A. and Morel, F. M.: Surface Complexation Modeling: Hydrous Ferric Oxide, Wiley, New York, 1990.

Elser, J. J., Bracken, M. E. S., Cleland, E. E., Gruner, D. S., Harpole, W. S., Hillebrand, H., Ngai, J. T., Seabloom, E. W., Shurin, J. B., and Smith, J. E.: Global analysis of nitrogen and phosphorus limitation of primary producers in freshwater, marine and terrestrial ecosystems, Ecol. Lett., 10, 1135–1142, doi:10.1111/j.1461-0248.2007.01113.x, 2007.

Fox, L. E.: A model for inorganic control of phosphate concentrations in river waters, Geochim. Cosmochim. Ac., 53, 417–428, 1989.

Frei, S., Knorr, K. H., Peiffer, S., and Fleckenstein, J. H.: Surface micro-topography causes hot spots of biogeochemical activity in wetland systems: a virtual modeling experiment, J. Geophys. Res.-Biogeo., 117, G00N12, doi:10.1029/2012JG002012, 2012.

Friedman, J. H.: A variable span scatterplot smoother, Laboratory for Computational Statistics, Stanford University, Stanford University Technical Report No. 5, 1984.

Gerke, J.: Phosphate adsorption by humic/Fe-oxide mixtures aged at pH 4 and 7 and by poorly ordered Fe-oxide, Geoderma, 59, 279–288, 1993.

Griffioen, J.: Extent of immobilisation of phosphate during aeration of nutrient-rich, anoxic groundwater, J. Hydrol., 320, 359–369, doi:10.1016/j.jhydrol.2005.07.047, 2006.

HESSD
11, 6637–6674, 2014

Griffioen, J., Vermooten, S., and Janssen, G.: Geochemical and palaeohydrological controls on the composition of shallow groundwater in the Netherlands, Appl. Geochem., 39, 129–149, doi:10.1016/j.apgeochem.2013.10.005, 2013.

Gunnars, A., Blomqvist, S., Johansson, P., and Andersson, C.: Formation of Fe(III) oxyhydroxide colloids in freshwater and brackish seawater, with incorporation of phosphate and calcium, Geochim. Cosmochim. Ac., 66, 745–758, 2002.

Hayashi, M., and Yanagi, T.: Water and phosphorus budgets in the Yellow River estuary including the submarine fresh groundwater, in: From Headwaters to the Ocean: Hydrological Change and Water Management – Proceedings of the International Conference on Hydrological Changes and Management from Headwaters to the Ocean, Hydrochange 2008, Kyoto, Japan, 1–3 October 2008, 665–668, 2009.

Holman, I. P., Whelan, M. J., Howden, N. J. K., Bellamy, P. H., Willby, N. J., Rivas-Casado, M., and McConvey, P.: Phosphorus in groundwater – an overlooked contributor to eutrophication?, Hydrol. Process., 22, 5121–5127, doi:10.1002/hyp.7198, 2008.

Horowitz, A. J.: Determining annual suspended sediment and sediment-associated trace element and nutrient fluxes, Sci. Total Environ., 400, 315–343, doi:10.1016/j.scitotenv.2008.04.022, 2008.

Houot, S. and Berthelin, J.: Submicroscopic studies of iron deposits occurring in field drains: formation and evolution, Geoderma, 52, 209–222, 1992.

House, W. A. and Denison, F. H.: Nutrient dynamics in a lowland stream impacted by sewage effluent: Great Ouse, England, Sci. Total Environ., 205, 25–49, doi:10.1016/S0048-9697(97)00086-7, 1997.

Hug, S. J. and Leupin, O.: Iron-catalyzed oxidation of arsenic(iii) by oxygen and by hydrogen peroxide: pH-dependent formation of oxidants in the Fenton reaction, Environ. Sci. Technol., 37, 2734–2742, doi:10.1021/es026208x, 2003.

Jordan, P., Melland, A. R., Mellander, P. E., Shortle, G., and Wall, D.: The seasonality of phosphorus transfers from land to water: implications for trophic impacts and policy evaluation, Sci. Total Environ., 434, 101–109, 2012.

Kaegi, R., Voegelin, A., Folini, D., and Hug, S. J.: Effect of phosphate, silicate, and Ca on the morphology, structure and elemental composition of Fe(III)-precipitates formed in aerated Fe(II) and As(III) containing water, Geochim. Cosmochim. Ac., 74, 5798–5816, doi:10.1016/j.gca.2010.07.017, 2010.

HESSD

11, 6637–6674, 2014

Krause, S., Heathwaite, L., Binley, A., and Keenan, P.: Nitrate concentration changes at the groundwater-surface water interface of a small Cumbrian river, Hydrol. Process., 23, 2195–2211, 2009.
Lienemann, C. P., Monnerat, M., Janusz, D., and Perret, D.: Identification of stoichiometric iron-phosphorus colloids produced in a eutrophic lake, Aquat. Sci., 61, 133–149, 1999.
Lofts, S., Tipping, E., and Hamilton-Taylor, J.: The chemical speciation of Fe(III) in freshwaters, Aquat. Geochem., 14, 337–358, doi:10.1007/s10498-008-9040-5, 2008.
Lyvén, B., Hassellöv, M., Turner, D. R., Haraldsson, C., and Andersson, K.: Competition between iron- and carbon-based colloidal carriers for trace metals in a freshwater assessed using flow field-flow fractionation coupled to ICPMS, Geochim. Cosmochim. Ac., 67, 3791–3802, doi:10.1016/S0016-7037(03)00087-5, 2003.
Maassen, S. and Balla, D.: Impact of hydrodynamics (ex- and infiltration) on the microbially controlled phosphorus mobility in running water sediments of a cultivated northeast German wetland, Ecol. Eng., 36, 1146–1155, doi:10.1016/j.ecoleng.2010.01.009, 2010.
Macrae, M. L., Zhang, Z., Stone, M., Price, J. S., Bourbonniere, R. A., and Leach, M.: Subsurface mobilization of phosphorus in an agricultural riparian zone in response to flooding from an upstream reservoir, Can. Water Resour. J., 36, 293–311, doi:10.4296/cwrj3604810, 2011.
Mayer, T. D. and Jarrell, W. M.: Phosphorus sorption during iron(II) oxidation in the presence of dissolved silica, Water Res., 34, 3949–3956, doi:10.1016/S0043-1354(00)00158-5, 2000.
Meng, X., Korfiatis, G. P., Bang, S., and Bang, K. W.: Combined effects of anions on arsenic removal by iron hydroxides, Toxicol. Lett., 133, 103–111, doi:10.1016/S0378-4274(02)00080-2, 2002.
Neal, C., Jarvie, H. P., Williams, R. J., Neal, M., Wickham, H., and Hill, L.: Phosphorus – calcium carbonate saturation relationships in a lowland chalk river impacted by sewage inputs and phosphorus remediation: an assessment of phosphorus self-cleaning mechanisms in natural waters, Sci. Total Environ., 282–283, 295–310, doi:10.1016/S0048-9697(01)00920-2, 2002.
Neal, C., Lofts, S., Evans, C. D., Reynolds, B., Tipping, E., and Neal, M.: Increasing Iron Concentrations in UK Upland Waters, Aquat. Geochem., 14, 263–288, doi:10.1007/s10498-008-9036-1, 2008.
Parkhurst, D. L. and Appelo, C.: User's Guide to PHREEQC (Version 2): a Computer Program for Speciation, Batch-Reaction, One-Dimensional Transport, and Inverse Geochemical Calculations, Denver, Colorado, United States, U.S. Geological Survey, 1999.

HESSD
11, 6637–6674, 2014

Perry, R. H., Green, D. W., and Maloney, J. O.: Perry's Chemical Engineers' Handbook, McGraw-Hill Education, New York, 1997.
Reddy, K. R., Kadlec, R. H., Flaig, E., and Gale, P. M.: Phosphorus retention in streams and wetlands: a review, Crit. Rev. Env. Sci. Tec., 29, 83–146, 1999.
Roberts, L. C., Hug, S. J., Ruettimann, T., Billah, M., Khan, A. W., and Rahman, M. T.: Arsenic removal with iron(ii) and iron(iii) in waters with high silicate and phosphate concentrations, Environ. Sci. Technol., 38, 307–315, 2004.
Rozemeijer, J. C., Van Der Velde, Y., De Jonge, H., Van Geer, F., Broers, H. P., and Bierkens, M.: Application and evaluation of a new passive sampler for measuring average solute concentrations in a catchment scale water quality monitoring study, Environ. Sci. Technol., 44, 1353–1359, 2010a.
Rozemeijer, J. C., Van Der Velde, Y., Van Geer, F. C., De Rooij, G. H., Torfs, P. J. J. F., and Broers, H. P.: Improving load estimates for NO_3 and P in surface waters by characterizing the concentration response to rainfall events, Environ. Sci. Technol., 44, 6305–6312, 2010b.
Rozemeijer, J. C., Van Der Velde, Y., McLaren, R. G., Van Geer, F. C., Broers, H. P., and Bierkens, M. F. P.: Integrated modeling of groundwater-surface water interactions in a tile-drained agricultural field: the importance of directly measured flow route contributions, Water Resour. Res., 46, W11537, doi:10.1029/2010WR009155, 2010c.
Scanlon, T. M., Kiely, G., and Amboldi, R.: Model determination of non-point source phosphorus transport pathways in a fertilized grassland catchment, Hydrol. Process., 19, 2801–2814, 2005.
Sharpley, A. N., Kleinman, P. J. A., Heathwaite, A. L., Gburek, W. J., Folmar, G. J., and Schmidt, J. P.: Phosphorus loss from an agricultural watershed as a function of storm size, J. Environ. Qual., 37, 362–368, 2008.
Shenker, M., Seitelbach, S., Brand, S., Haim, A., and Litaor, M. I.: Redox reactions and phosphorus release in re-flooded soils of an altered wetland, Eur. J. Soil Sci., 56, 515–525, 2005.
Spiteri, C., Regnier, P., Slomp, C. P., and Charette, M. A.: pH-dependent iron oxide precipitation in a subterranean estuary, J. Geochem. Explor., 88, 399–403, doi:10.1016/j.gexplo.2005.08.084, 2006.
Stumm, W. and Lee, G. F.: Oxygenation of Ferrous Iron, Ind. Eng. Chem., 53, 143–146, doi:10.1021/ie50614a030, 1961.
Sung, W. and Morgan, J. J.: Kinetics and product of ferrous iron oxygenation in aqueous systems, Environ. Sci. Technol., 14, 561–568, doi:10.1021/es60165a006, 1980.

HESSD
11, 6637–6674, 2014

Van Beek, C. G. E. M., Breedveld, R. J. M., Juhász-Holterman, M., Oosterhof, A., and Stuyfzand, P. J.: Cause and prevention of well bore clogging by particles, Hydrogeol. J., 17, 1877–1886, 2009.
Van den Eertwegh, G. A. P. H.: Water and Nutrient Budgets at Field and Regional Scale, Travel Times of Drainage Water and Nutrient Loads to Surface Water, Ph.D. thesis, Wageningen University, 2002.
Van der Velde, Y., Rozemeijer, J. C., de Rooij, G. H., van Geer, F. C., and Broers, H. P.: Field-scale measurements for separation of catchment discharge into flow route contributions, Vadose Zone J., 9, 25–35, doi:10.2136/vzj2008.0141, 2010.
Van Geen, A., Robertson, A. P., and Leckie, J. O.: Complexation of carbonate species at the goethite surface: implications for adsorption of metal ions in natural waters., Geochim. Cosmochim. Ac., 58, 2073–2086, 1994.
Vanlierde, E., De Schutter, J., Jacobs, P., and Mostaert, F.: Estimating and modeling the annual contribution of authigenic sediment to the total suspended sediment load in the Kleine Nete Basin, Belgium, Sediment. Geol., 202, 317–332, doi:10.1016/j.sedgeo.2007.05.003, 2007.
Vermooten, J. S. A., Maring, L., Van Vliet, M. E., and Griffioen, J.: Nationwide, geological characterization of regional groundwater composition in the geotop of Netherlands., TNO, Utrecht, the Neterlands, TNO-report 2006-U-R171/A, 2006.
Voegelin, A., Senn, A. C., Kaegi, R., Hug, S. J., and Mangold, S.: Dynamic Fe-precipitate formation induced by Fe(II) oxidation in aerated phosphate-containing water, Geochim. Cosmochim. Ac., 117, 216–231, 2013.
Vollrath, S., Behrends, T., and van Cappellen, P.: Oxygen dependency of neutrophilic Fe(II) oxidation by Leptothrix differs from abiotic reaction, Geomicrobiol. J., 29, 550–560, 2012.
von Gunten, U. and Schneider, W.: Primary products of the oxygenation of iron(II) at an oxic – anoxic boundary: nucleation, aggregation, and aging, J. Colloid Interf. Sci., 145, 127–139, doi:10.1016/0021-9797(91)90106-I, 1991.
Walling, D. E., Collins, A. L., and Stroud, R. W.: Tracing suspended sediment and particulate phosphorus sources in catchments, J. Hydrol., 350, 274–289, 2008.
Wassen, M. J., Venterink, H. O., Lapshina, E. D., and Tanneberger, F.: Endangered plants persist under phosphorus limitation, Nature, 437, 547–550, 2005.
Withers, P. J. A. and Haygarth, P. M.: Agriculture, phosphorus and eutrophication: a European perspective, Soil Use Manage., 23, 1–4, doi:10.1111/j.1475-2743.2007.00116.x, 2007.

HESSD
11, 6637–6674, 2014

Wolthoorn, A., Temminghoff, E. J. M., Weng, L., and van Riemsdijk, W. H.: Colloid formation in groundwater: effect of phosphate, manganese, silicate and dissolved organic matter on the dynamic heterogeneous oxidation of ferrous iron, Appl. Geochem., 19, 611–622, doi:10.1016/j.apgeochem.2003.08.003, 2004.

HESSD
11, 6637–6674, 2014

Table 1. Averaged P and Fe concentrations and molar P/Fe ratios of the groundwater, the reservoir water during winter time and the drain 3 effluent.

	avg P $\mu mol\,L^{-1}$	avg Fe $\mu mol\,L^{-1}$	avg P/Fe ratio
groundwater 1	22.1	422	0.053
groundwater 2	5.6	353	0.016
groundwater 3	12.0	182	0.066
groundwater 4	14.6	184	0.079
drain 3 after Sep 2007	2.6	235	0.011
Reservoir 1 Nov–Feb	0.5	56	0.009
Reservoir 2 Nov–Feb	1.0	229	0.004
Reservoir 3 Nov–Feb	1.6	119	0.014

HESSD
11, 6637–6674, 2014

Table 2. Input parameters for the CSTR model.

	Fe inflow ($mg\,L^{-1}$)	PO_4 inflow ($mg\,L^{-1}$)	pH	pO_2 (atm)	T (°C)
Year average	14.5	0.33	6.4	0.21	9.3
Summer situation	10.6	0.19	6.6	0.1	17
Winter situation	21.3	0.52	6.2	0.21	5

HESSD
11, 6637–6674, 2014

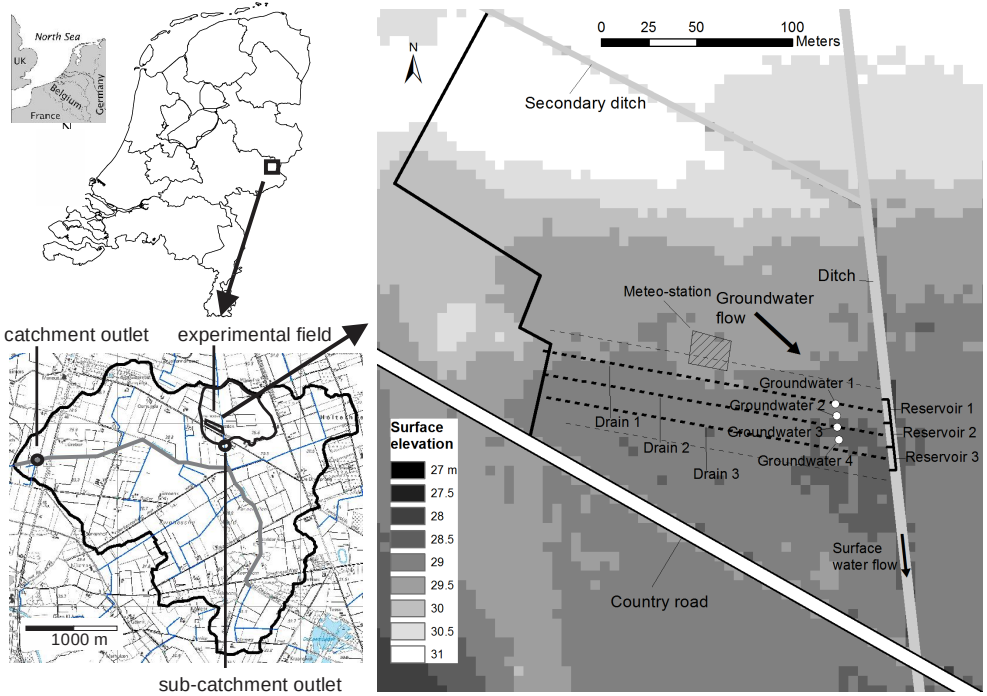

Figure 1. Location of the Hupsel catchment and the experimental field. The catchment map shows the sub-catchment outlet and catchment outlet. The field map shows the three measured tube drains, the four groundwater wells and the location of the in-stream reservoirs.

HESSD
11, 6637–6674, 2014

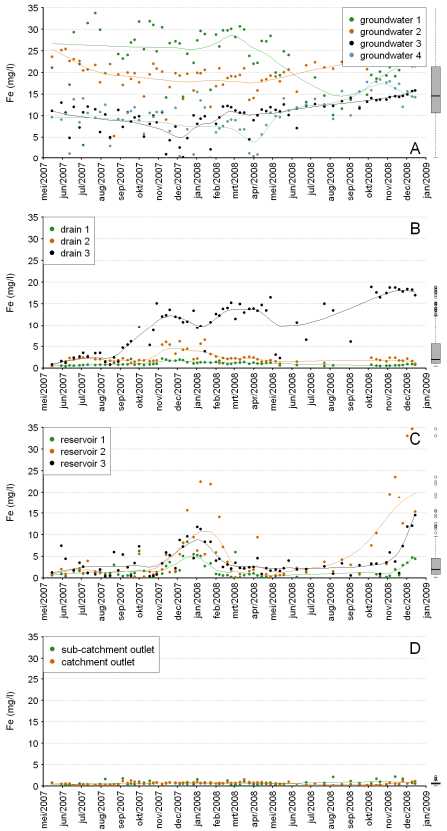

Figure 2. Time series and boxplots of Fe concentration of groundwater **(A)**, tube drain water **(B)**, in-stream reservoir water **(C)** and surface water **(D)**. The smoothing line through the measured data points is calculated with the method of Friedman (1984). The bold solid line within each box plot is the median concentration. The lower and upper side of the box represents the 0.25 and the 0.75 quantile. Whiskers extend to the maximum and minimum value unless the values are lager then 1.5 times the box length. Open circles are extreme values.

HESSD
11, 6637–6674, 2014

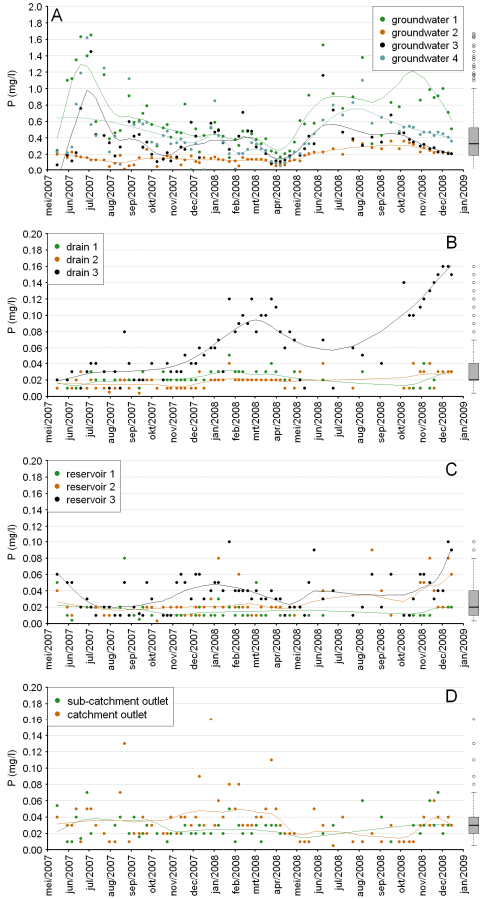

Figure 3. Time series and boxplots of dissolved total P concentrations of groundwater **(A)**, tube drain water **(B)**, in-stream reservoir water **(C)** and surface water **(D)**. **(B)**, **(C)** and **(D)** share the same y-axis. Remarks as for Fig. 2.

HESSD
11, 6637–6674, 2014

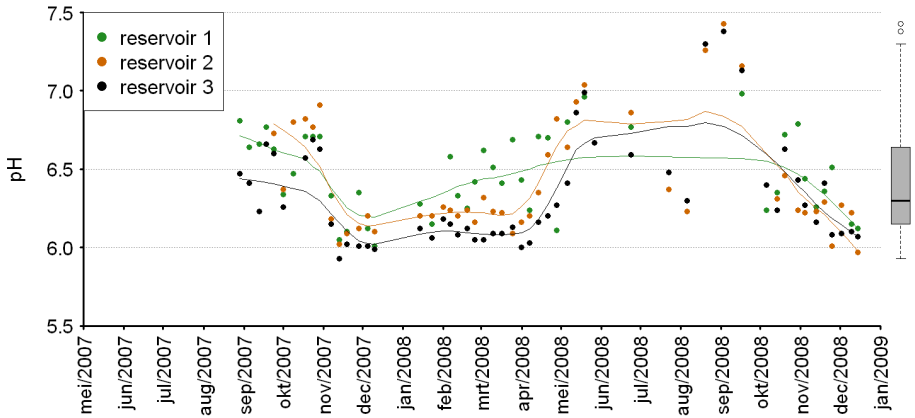

Figure 4. Time series of pH of groundwater. Remarks as for Fig. 2.

HESSD
11, 6637–6674, 2014

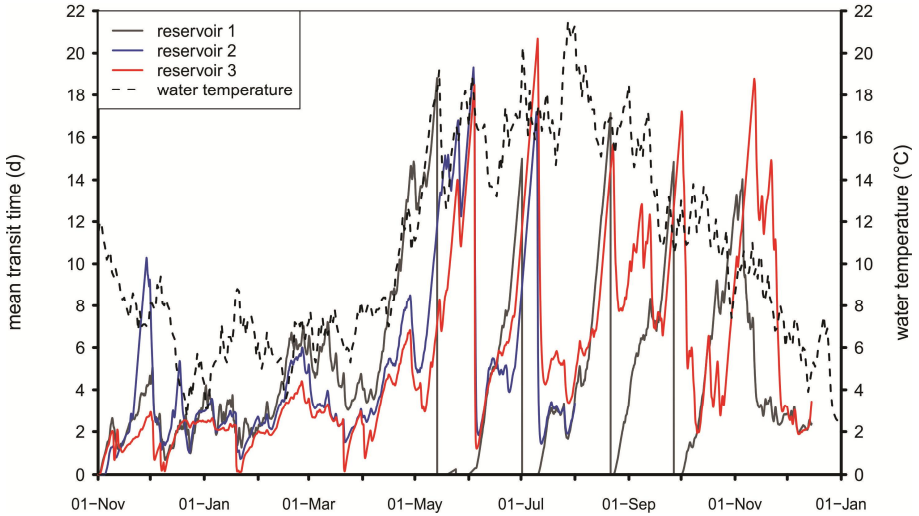

Figure 5. Mean transit time of the water insight the in-stream reservoirs and the temperature of the ditch water direct downstream the reservoirs.

HESSD
11, 6637–6674, 2014

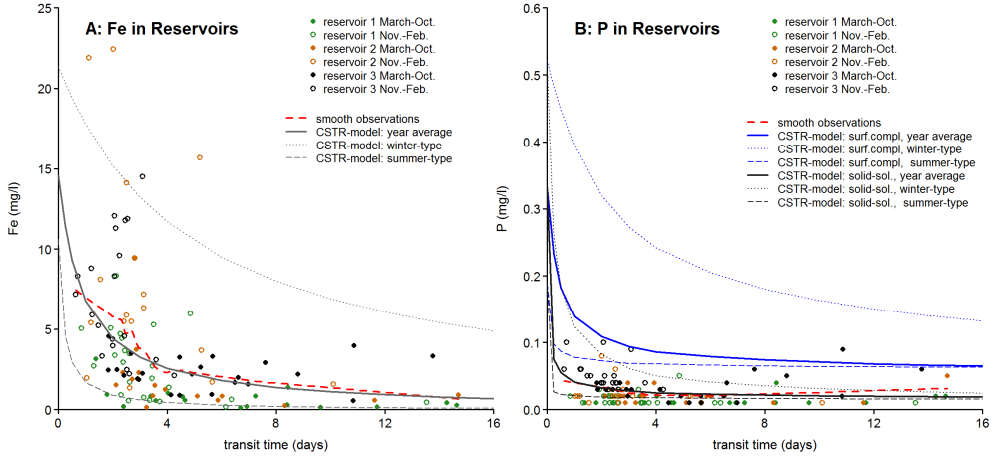

Figure 6. Measured Fe and P concentrations vs. the mean transit time of the water in the reservoirs. The blue and black lines show the steady-state Fe and P concentrations according to the CSTR-models as function of the transit time for the yearly average situation (T = 9.3 °C; pH = 6.4; pO_2 = 0.21), the winter-type conditions (T = 5 °C; pH = 6.2; pO_2 = 0.21 atm) and summer-type conditions (T = 17 °C; pH = 6.6; pO_2 = 0.1 atm).

HESSD
11, 6637–6674, 2014

Figure 7. Pictures of the field ditch in the late summer (left) and winter (right). The red sediment indicates the presence of iron-hydroxides in the winter situation. These were absent in summer

HESSD
11, 6637–6674, 2014